Sedimentation of Noncolloidal Bidisperse Suspensions

Man Ken Cheung
Dept. of Chemical Engineering, Hong Kong University of Science & Technology, Kowloon, Hong Kong

Robert L. Powell
Dept. of Chemical Engineering, University of California, Davis, CA 95616

Michael J. McCarthy
Dept. of Food Science and Technology, University of California, Davis, CA 95616

Gravity sedimentation of bidisperse suspensions is encountered in many industrial applications, such as separation of gravel and sands from mining fluids. The design procedures for these gravity settlers, thickeners and clarifiers are often far from optimal. This is in part due to the lack of convenient and noninvasive methods to measure settling velocities and concentration profiles. Furthermore, studies of suspensions consisting of mixed particle sizes, which more closely approximates real systems, are scarce.

Several earlier works on bidisperse suspensions of noncolloidal particles have attempted to formulate models to predict the settling velocity. Smith (1965), extending Happel's cell theory (Happel, 1958) for the settling of single-sized particles, predicted the right trends for the settling velocities with changing particle volume fraction, while underpredicting the actual velocities. Lockett and Al-Habbooby (1973) applied the Richardson and Zaki (1954) correlation for monodisperse particles to each population of particles in a bidisperse suspension. Their model overpredicted the settling velocities, as it did not account for interparticle collisions and interactions arising from the relative velocities of the various sized particles. Mirza and Richardson (1979) extended the model of Lockett and Al-Habbooby (1973) to a multisized particle system. They applied a correction factor to the predicted velocities to obtain better agreement with the experimental values; however, this correction factor is purely empirical, and is limited in its range of applicability. Selim et al. (1983) modified this model to account for interparticle interactions by replacing the fluid density in the expression for the Stokes velocity of species i with the average density of a suspension consisting of fluid and of particles smaller in size than species i. They found good agreement between their model and experiments for concentrated suspensions having $0.12 \leq \phi_0 \leq 0.45$ where ϕ_0 is the initial concentration of the suspension. Recently, Davis and Gecol (1994) proposed a model for which the only parameters required are the dimensionless sedimentation coefficients of Batchelor and Wen (1982). The model agrees with Batchelor's theory (1982) in the dilute concentration limit ($\phi_0 \ll 0.1$), and it reduces to the Richardson and Zaki (1954) correlation for monodisperse suspensions. Settling velocity predictions are in good agreement with measurements for both dilute and concentrated suspensions.

During sedimentation in bidisperse suspensions consisting of particles of different sizes with the same density, two distinct regions are formed between the sediment at the bottom and the supernatant liquid at the top. The lower suspension region has uniform concentration, and it contains particles of both sizes. Whereas, the upper uniform concentration region consists only of the small particles. The interface between the upper and lower suspension regions, and the interface between the supernatant liquid and the upper suspension region are not sharp at low volume fractions ($\phi_0 < 0.15$) because of spreading in particle sizes about the two mean diameters. Measurements of the interface settling velocity by conventional visual methods would lead to uncertainties. We circumvent this problem by using nuclear magnetic resonance imaging (NMRI) to monitor the entire batch sedimentation process of a bidisperse system. NMRI provides a quick and noninvasive way to measure particle volume fraction within a suspension as a function of time and position (Turney et al., 1995a,b). From the concentration profiles, we determine the median velocity $U_{1/2}$ and regard it as the interface settling velocity. The median velocity is defined as the average fall rate over a distance of the isoconcentration plane at which its concentration is half-way between that below and that above the interface (Davis and Birdsell, 1988). The median velocity of a suspension with a slight spread in particle size is almost identical to the settling velocity at the same volume fraction of a single-sized suspension that has all particles with diame-

Correspondence concerning this article should be addressed to M. J. McCarthy.

ters equal to the mean diameter of the multisized suspension (Davis and Hassen, 1988).

Models

The important working equations in the model of Selim et al. (1983) for a bidisperse suspension are:

$$U_{1,2} = U_{s,1,2}(1-\phi_{1,2}) - U_{s,2,2}\phi_{2,2} \quad (1)$$

$$U_{2,2} = U_{s,2,2}(1-\phi_{2,2}) - U_{s,1,2}\phi_{1,2} \quad (2)$$

$$U_{1,1} = U_{s,1,1}(1-\phi_{1,1}) \quad (3)$$

$$\phi_{1,1} = \phi_{1,2}\frac{(U_{2,2}-U_{1,2})}{(U_{2,2}-U_{1,1})} \quad (4)$$

where $U_{s,i,j}$ is the slip velocity (fluid-particle relative average velocity) and $U_{i,j}$ is the settling velocity for particle species i in suspension region j; $i=1$ refers to the small particles and $j=1$ refers to the upper suspension region. The upper interface settling velocity $U_{1/2,\text{ upper}}$ is $U_{1,1}$, and the lower interface settling velocity $U_{1/2\text{ lower}}$ is $U_{2,2}$. Equation 4 is the jump mass balance for the small particles at the interface that separates the upper and the lower uniform concentration regions. Since $U_{1,2} < U_{1,1}$ as a result of larger hindered settling effects in the lower region, $\phi_{1,1} > \phi_{1,2}$. The slip velocities are given by a Richardson- and Zaki-type correlation proposed by Garside and Al-Dibouni (1977). Sellim et al. (1983) also replaced the fluid density in the Stokes velocity expression for the large particles with an effective density of a suspension consisting of the fluid and the smaller-sized particles.

The Davis and Gecol (1994) model uses the sedimentation coefficients determined from Batchelor (1982). The settling velocities are expressed as:

$$U_{i,j} = U_{o,i}(1-\phi_j)^{-S_{ii}}\left[1+\sum_{k\neq i}(S_{ik}-S_{ii})(\phi_{k,j})\right] \quad (5)$$

where $\phi_j = \Sigma(\phi_{k,j})$ is the total particle volume fraction in the jth suspension region. For equidensity noncolloidal particles that are settling at large Peclet number and at low Reynolds number, $S_{11} = S_{22} = -5.6$, and S_{ik} is given by (Batchelor, 1982):

$$S_{ik} = -3.50 - 1.10\lambda - 1.02\lambda^2 - 0.002\lambda^3 \quad \text{for} \quad 0 \le \lambda \le 8 \quad (6)$$

where $\lambda = d_k/d_i$, the ratio of the mean diameters of two particle species.

In a typical computation, we begin with a homogeneous suspension of known volume fractions for the large and small particles, $\phi_{1,2}$ and $\phi_{2,2}$, respectively. The velocities $U_{1,2}$ and $U_{2,2}$ can then be calculated from Eqs. 1 and 2 or from Eq. 5, depending on the chosen model. An initial $\phi_{1,1}$ is assumed such as $\phi_{1,1} = \phi_{1,2}$. Equations 3 or 5, and 4 are then solved simultaneously by iterations for $U_{1,1}$ and $\phi_{1,1}$.

As shown below, the Selim et al. (1983) model and the Davis and Gecol (1994) model overpredict our data for semidilute concentrations ($\phi_0 < 0.15$). Previously, we observed that the Barnea and Mizrahi (1973) correlation agrees well with our measured hindered settling velocities for monodisperse suspensions in the creeping flow range (Turney et al., 1995b). Instead of the Garside and Al-Dibouni (1977) correlation used by Selim et al. (1983), we modified the Barnea and Mizrahi (1973) correlation to calculate the slip velocities. The effective suspension density of the lower and the upper region are, respectively:

$$\rho_{s,\text{lower}} = (1-\phi_{2,2}-\phi_{1,2})\rho_f + \phi_{2,2}\rho_2 + \phi_{1,2}\rho_1 \quad (7)$$

$$\rho_{s,\text{upper}} = (1-\phi_{1,1})\rho_f + \phi_{1,1}\rho_1 \quad (8)$$

which are used to account for the hydrostatic effect. The driving force is:

$$F_g = \frac{1}{6}\pi d_i^3(\rho_i - \rho_s)g$$

The drag force is increased by the momentum transfer hindrance and by the wall effect (Barnea and Mizrahi, 1973):

$$F_D = 3\pi d_i \mu_f U_{s,i,j}(1+\phi_o^{1/3})\exp\left[\frac{5\phi_0}{3(1-\phi_0)}\right]$$

Applying the force balance, we obtain

$$U_{s,i,j} = \frac{d_i^2(\rho_i-\rho_s)g}{18\mu_f}\frac{1}{(1+\phi_{1,1}^{1/3})\exp\left(\frac{5(\phi_{1,1})}{3(1-\phi_{1,1})}\right)}$$

Rearranging Eqs. 7 and 8 to express $(\rho_i - \rho_s)$ in terms of the volume fractions, the particle densities, and the fluid density, the settling velocities can then be expressed as:

$$U_{1/2,\text{ lower}} = U_{0,2}\left\{\frac{\left(1-\phi_{2,2}-\left(\frac{\rho_1-\rho_f}{\rho_2-\rho_f}\right)\phi_{1,2}\right)}{(1+\phi_0^{1/3})\exp\left(\frac{5\phi_0}{3(1-\phi_0)}\right)}\right\}(1-\phi_{2,2}) - U_{0,1}\left\{\frac{\left(1-\phi_{1,2}-\left(\frac{\rho_2-\rho_f}{\rho_1-\rho_f}\right)\phi_{2,2}\right)}{(1+\phi_0^{1/3})\exp\left[\frac{5\phi_0}{3(1-\phi_0)}\right]}\right\}\phi_{1,2} \quad (9)$$

Table 1. Physical Properties of Particles and Suspending Fluid

Particle	Mean Dia. (μm)	Spread s_i/d_i	Density (kg/m^3)
Type I	274	0.17	1.018×10^3
Type II	655	0.30	1.044×10^3
Type III	488	0.06	1.050×10^3

Suspending Fluid	Viscosity (mPa·s)	Density (kg/m^3)
(79 wt. % UCON 50-HB-55 21 wt. % UCON 75-h-90,000)	42.7	0.973×10^3

Table 2. Fourier Spin-Echo Pulse Sequence Parameters

Parameter	Value	Units
Predelay time	200	ms
Echo time	15	ms
In-plane resolution	256	points
Read-out gradient strength	425	Hz/mm
For 0.6-T General Electric CSI Experiments		
Field of view	180.99	mm
Number of acquisition	16	-
No slice-selection		
For 2-T General Electric CSI Experiments		
Field of view	60.33	mm
Number of acquisition	4	-
Slice thickness	10	mm
Slice-selection method:		
One-lobe sinc pulse with a trapezoidal gradient shape		

$$U_{1/2,\,\text{upper}} = U_{0,1}\left\{\frac{(1-\phi_{1,1})^2}{(1+\phi_{1,1}^{1/3})\exp\left[\dfrac{5(\phi_{1,1})}{3(1-\phi_{1,1})}\right]}\right\} \quad (10)$$

The Stokes velocity for the species i is given by:

$$U_{o,i} = \frac{d_i^2(\rho_i - \rho_f)g}{18\mu_f} \quad (11)$$

Experimental

Three particle sizes of polystyrene beads (Polysciences, Inc., Warrington, PA) were used. Particle-size distributions were measured with optical and scanning electronic microscopes. The uncertainty in mean particle diameter measurements is ± 1.5 μm. Particle densities were determined with a pycnometer, and the uncertainty is ± 1 kg/m^3. The suspending fluid was a blend of 79 wt. % UCON 50-HB-55 and 21 wt. % UCON 75-H-90,000 polyalkylene glycols (Union Carbide Corp., Danbury, CT). The fluid viscosity was measured at 21.5°C with a Cannon-Ubbelohde dilution type viscometer. Properties of the particles and the fluid are listed in Table 1.

Two types of sedimentation vessels were used: (1) Plexiglas cylinder with internal diameter of 4.5 cm and length of 16 cm; (2) Plexiglas cube with interior dimensions of 4.5 cm. The cylindrical vessel was for batch sedimentation experiments on monodisperse and bidisperse suspensions of Type I and Type II particles carried out in a 0.6-T General Electric CSI imaging spectrometer (Fremont, CA). Bidisperse suspensions of equal initial volume fractions of Type I and Type II particles were examined, that is, $\phi_{1,2} = \phi_{2,2} = \phi_0/2$. The cubic vessel was for monodisperse sedimentation experiments of Type III particles carried out in a 2-T General Electric CSI imaging spectrometer (Turney et al., 1995b). The experimental parameters for NMRI are listed in Table 2.

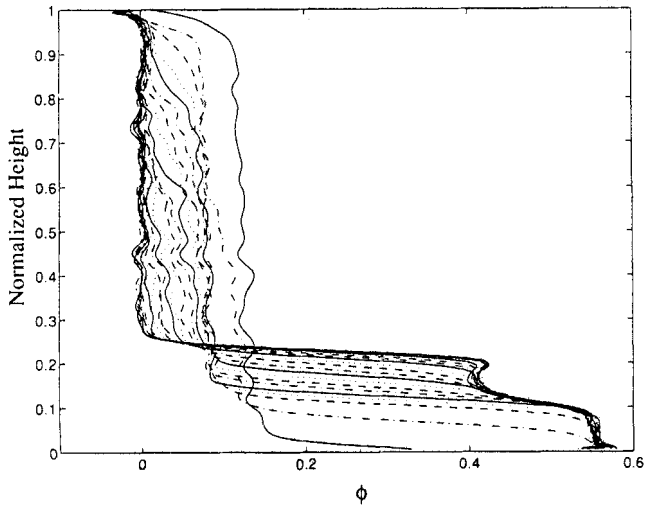

Figure 1. Normalized height vs. volume fraction for typical bidisperse suspension.

Profiles are shown at 278.2 s intervals with interfacial broadening; uniform concentration regions at 0.125 and 0.072 are distinguished.

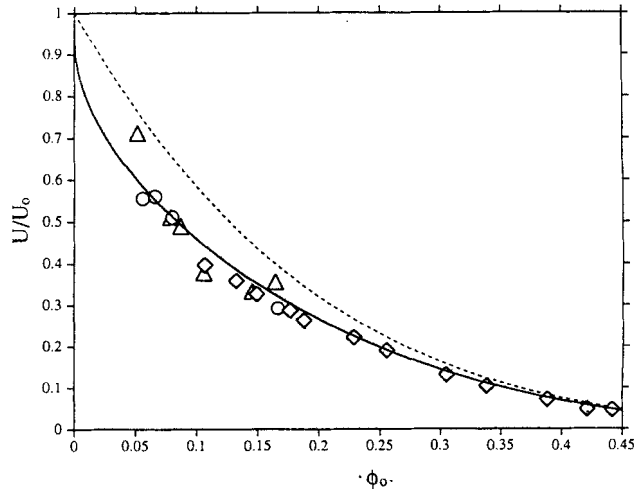

Figure 2. Comparison of NMRI-measured hindered settling functions of monodisperse suspensions with others.

Richardson and Zaki (1954) correlation with power index, n, 5.1 (- - - -); Barnea and Mizrahi (1973) correlation (——). The latter correlation agrees well with NMRI-measured data. Data for Types I (Δ), II (○), and III (◇) particles are also shown.

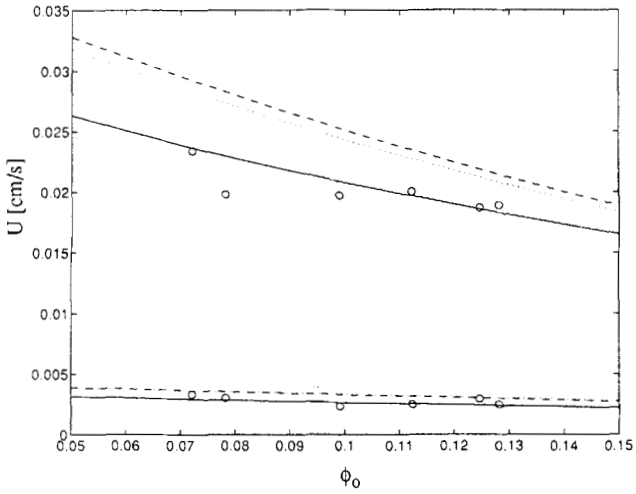

Figure 3a. NMRI-measured settling velocity vs. total initial volume fraction of bidisperse suspensions.

...., calculations using Selim et al. (1983); ----, calculations from Davis and Gecol (1994); ——, calculations from our model.

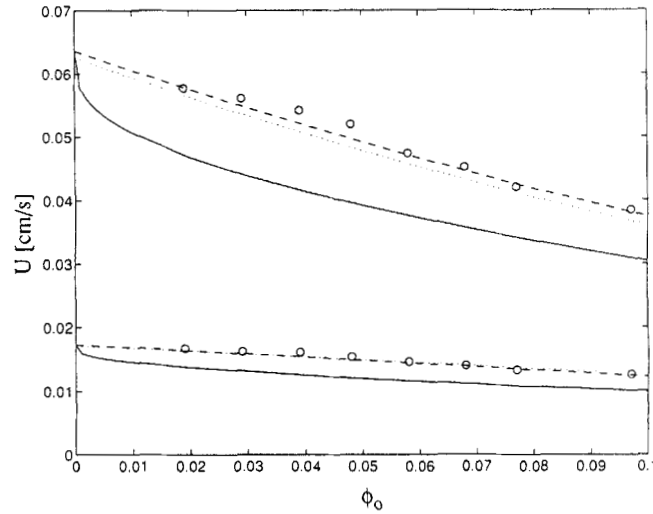

Figure 4a. Settling velocity vs. total initial volume fraction of bidisperse suspensions data from Davis and Birdsell (1988).

...., Selim et al. (1983); ----, Davis and Gecol (1994); ——, our model.

NMRI experiments were carried out in the bore of a superconducting magnet housed in an air-conditioned room at 21°C. No special setup was used to monitor the temperature of the fluid. However, the fluid had been in the room for many days, and so its temperature was regarded the same as the ambient temperature. Air temperature variations within the bore of the magnet were found to be less than 1°C over 24 h. NMRI measurements of the suspending fluid were made prior to each sedimentation experiment. This blank sample was placed at the same location inside the magnet as the suspension sample. Because signal intensities are proportional to the mobile hydrogen nuclei density of the suspending fluid, the particle volume fraction ϕ is given by:

$$\phi(h,t) = 1 - \frac{S_s(h,t)}{S_b(h)} \tag{12}$$

where S_b and S_s are the signal intensities along the vertical axis of the vessel for the blank and sedimenting suspension samples, respectively. The spin-lattice and the spin-spin relaxation times ($T_1 = 340$ ms and $T_2 = 70$ ms, respectively) were found to be independent of ϕ, and so Eq. 12 allows for a complete description of ϕ as a function of height measured from the top of the supernatant liquid h and time t.

Results and Discussion

Figure 1 shows the NMRI-measured time evolution of the normalized height vs. volume fraction profile for a typical bidisperse suspension. The upper and lower uniform suspen-

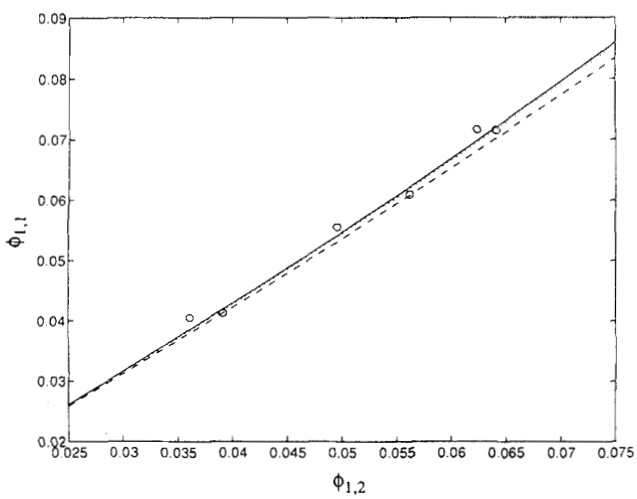

Figure 3b. Small-particle volume fraction in the upper suspension region, $\phi_{1,1}$, vs. that in the lower region, $\phi_{1,2}$.

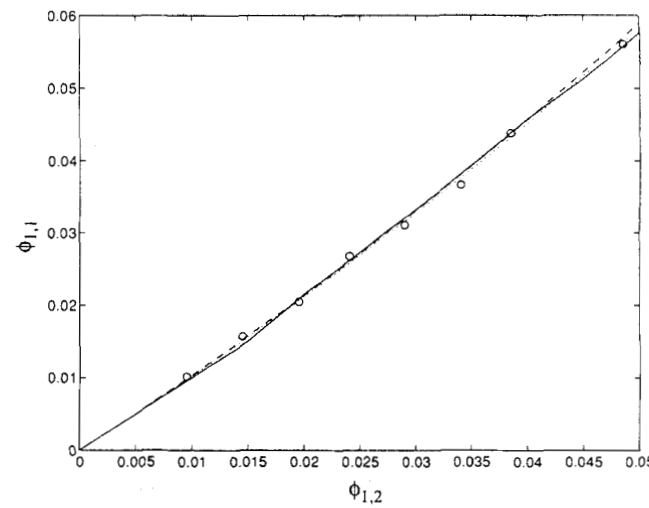

Figure 4b. Small-particle volume fraction in the upper suspension region, $\phi_{1,1}$, vs. that in the lower region, $\phi_{1,2}$.

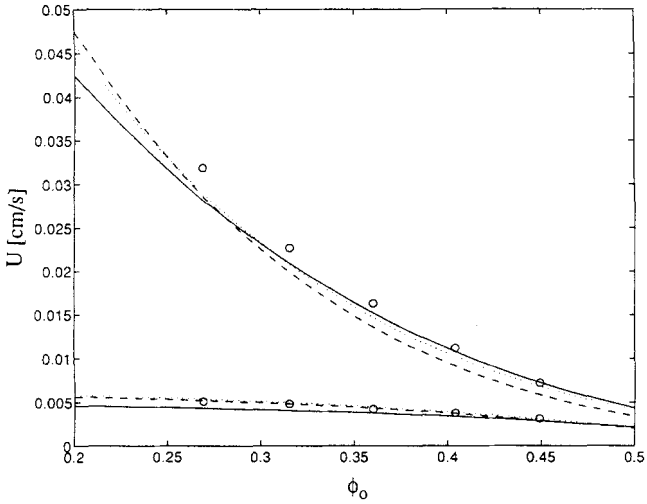

Figure 5. Settling velocity vs. total initial volume fraction of bidisperse suspensions.

Data taken from Figure 2 of Mirza and Richardson's article (1979). $\phi_{1,2}$ was fixed at 0.068, but $\phi_{2,2}$ was varied from 0.20 to 0.38. At these high total concentrations, settling velocities predicted by these three models are similar.

sion regions are clearly distinguishable. There are interfacial broadening at the upper and lower interfaces due to dispersity in particle sizes (Turney et al., 1995b).

For monodisperse systems, the measured hindered settling function follows closely the Barnea and Mizrahi (1973) correlation, Figure 2. The Richardson and Zaki (1954) correlation with power index $n = 5.1$ approaches the Barnea and Mizrahi (1973) correlation at $\phi_0 > 0.40$. At $\phi_0 < 0.15$, the two correlations have the largest differences.

As shown in Figure 3a, our model predicts our experimental data well, but the Selim et al. (1983) model and the Davis and Gecol (1994) model do not. All three models, however, predict almost identical concentrations of the small particles in the upper region $\phi_{1,1}$ as shown in Figure 3b. On the other hand, both the Selim et al. model and the Davis and Gecol model predict the data of Davis and Birdsell (1988) well, but ours does not (Figure 4a). All three models also predict about the same $\phi_{1,1}$ in Figure 4b. At higher concentrations, all three models predict values very close to the measured settling velocities (Mirza and Richardson, 1979) (Figure 5).

The Selim et al. (1983) model and the Davis and Gecol (1994) model are extensions of the Richardson and Zaki (1954) model and the Batchelor (1982) model, which assume a random distribution of suspended particles. Our modified Barnea and Mizrahi model like its original version assumes an ordered microstructure in particle suspensions. This difference yields large differences in the predicted velocities at low concentrations. It is unclear from the literature what are the factors that determine a suspension having a random vs. an ordered microstructure (Davis and Acrivos, 1985).

Figures 6a and 6b show the settling velocity $U_{1/2}$ vs. time for $\phi_0 = 0.072$ and $\phi_0 = 0.099$, respectively. The steady state $U_{1/2}$ is lower at high concentration than at low concentration, and the higher concentration suspension requires less time to reach steady state because of a larger hindered settling effect. When the large particles are completely settled, the small particles will then reach steady-state fall velocities. When large particles settle in a suspension of small particles, they displace not only the fluid but also the smaller-sized particles (Selim et al., 1983). The settling velocities of large particles in our bidisperse systems such as $U_{1/2,\,\text{lower}}(\phi_{2,2} = 0.056) = 0.0200$ cm/s, are smaller than those of their monodisperse counterparts at the same volume fraction such as $U_{1/2}(\phi_0 = 0.056) = 0.0234$ cm/s. The initial $U_{1/2,\,\text{upper}}$ for the small particles might have been kept low due to the small particles being displaced upward into the upper region by the settling large particles. Once complete separation between the two types of particle had occurred, $U_{1/2,\,\text{upper}}$ becomes independent of the large particles, and it can be expressed as a function of $\phi_{1,1}$.

Acknowledgment

We would like to thank Dr. R. J. Kauten for his assistance with the NMRI spectrometers. This work was supported by National Science Foundation Award CTS-9057660.

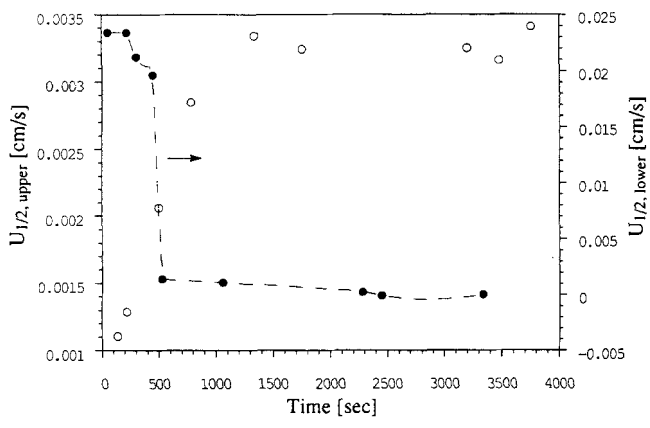

Figure 6. Time evolution of settling velocities for (a) $\phi_o = 0.072$, and (b) $\phi_o = 0.099$ bidisperse suspensions.

Upper interface settling velocity (○) is read from the left axis of ordinates; lower interface settling velocity (●) is read from the right axis of ordinates.

Notation

d_i = mean particle diameter of species i
g = acceleration due to gravity
s_i = standard deviation in particle diameter of species i
S_b = NMRI signal intensity of blank (pure suspending fluid)
S_s = NMRI signal intensity of suspension
S_{ii}, S_{ik} = sedimentation coefficients
U = hindered settling velocity
$U_{o,i}$ = Stokes velocity of species i

Greek letters

μ_f = viscosity of suspending fluid
ρ_f = density of suspending fluid
ρ_i = density of species i
ρ_s = effectve suspension density
ϕ_0 = total initial particle volume fraction

Subscripts

i = particle species i, where i is numbered successively starting with smallest species
j = suspension region j, where j is numbered successively starting with topmost region

Literature Cited

Barnea, E., and J. Mizrahi, "A Generalized Approach to the Fluid Dynamics of Particulate Systems: I. General Correlation for Fluidization and Sedimentation in Solid Multiparticle Systems," *Chem. Eng. J.*, **5**, 171 (1973).

Batchelor, G. K., "Sedimentation in a Dilute Polydisperse System of Interacting Spheres: 1. General Theory," *J. Fluid Mech.*, **119**, 379 (1982).

Batchelor, G. K., and C. S. Wen, "Sedimentation in a Dilute Polydisperse System of Interacting Spheres: 2. Numerical Results," *J. Fluid Mech.*, **124**, 495 (1982).

Davis, R. H., and A. Acrivos, "Sedimentation of Noncolloidal Particles at Low Reynolds Numbers," *Ann. Rev. Fluid Mech.*, **17**, 91 (1985).

Davis, R. H., and K. H. Birdsell, "Hindered Settling of Semidilute Monodisperse and Polydisperse Suspensions," *AIChE J.*, **34**, 123 (1988).

Davis, R. H., and H. Gecol, "Hindered Settling Function with No Empirical Parameters for Polydisperse Suspensions," *AIChE J.*, **40**, 570 (1994).

Davis, R. H., and M. A. Hassen, "Spreading of the Interface at the Top of a Slightly Polydisperse Sedimenting Suspensions," *J. Fluid Mech.*, **196**, 107 (1988).

Garside, J., and M. R. Al-Dibouni, "Velocity-voidage Relationship for Fluidization and Sedimentation in Solid-liquid Systems.," *Ind. Eng. Chem. Process Des. Dev.*, **16**, 206 (1977).

Happel, J., "Viscous Flow in Multiparticle Systems: Slow Motion of Fluids Relative to Bed of Spherical Particles," *AIChE J.*, **4**, 197 (1958).

Lockett, M. J., and H. M. Al-Habbooby, "Differential Settling by Size of Two Particle Species in a Liquid," *Trans. Inst. Chem. Eng.*, **51**, 281 (1973).

Mirza, S., and J. F. Richardson, "Sedimentation of Suspensions of Particles of Two or More Sizes," *Chem. Eng. Sci.*, **34**, 447 (1979).

Richardson, J. F., and W. N. Zaki, "Sedimentation and Fluidization: Part I," *Trans. Inst. Chem. Eng.*, **32**, 35 (1954).

Selim, M. S., A. C. Kothari, and R. M. Turian, "Sedimentation of Multisized Particles in Concentrated Suspensions," *AIChE J.*, **29**, 1029 (1983).

Smith, T. N., "The Differential Sedimentation of Particles of Two Different Species," *Trans. Inst. Chem. Eng.*, **43**, T69 (1965).

Turney, M. A., M. K. Cheung, R. L. Powell, and M. J. McCarthy, "Hindered Settling of Rod-Like Particles Measured with Magnetic Resonance Imaging," *AIChE J.*, **41**, 251 (1995a).

Turney, M. A., M. K. Cheung, M. J. McCarthy, and R. L. Powell, "Magnetic Resonance Imaging Study of Sedimenting Suspensions of Noncolloidal Spheres," *Phys. Fluids*, **7**, 904 (1995b).

Manuscript received Apr. 4, 1994, and revision received Jan. 23, 1995.